Article

Crustal carbonate build-up as a driver for Earth's oxygenation

Lewis J. Alcott [1,2,3,9] ✉, **Craig Walton** [4,5,6], **Noah J. Planavsky** [2], **Oliver Shorttle** [4,7] & **Benjamin J. W. Mills** [8]

Oxygenation of Earth's atmosphere and oceans played a pivotal role in the evolution of the surface environment and life. It is thought that the rise in oxygen over Earth's history was driven by an increasing availability of the photosynthetic limiting nutrient phosphate combined with declining oxygen-consuming inputs from the mantle and crust. However, it has been difficult to assess whether these processes alone can explain Earth's oxygenation history. Here we develop a theoretical framework for the long-term global oxygen, phosphorus and carbon cycles, incorporating potential trajectories for the emergence of continents, the degassing of mantle volatiles and the resulting increase in the size of the crustal carbonate reservoir. We find that we can adequately simulate the Earth's oxygenation trajectory in both the atmosphere and oceans, alongside reasonable reconstructions of planetary temperature, atmospheric carbon dioxide concentration, phosphorus burial records and carbon isotope ratios. Importantly, this is only possible when we include the accumulation of carbonates in the crust, which permits ever-increasing carbon recycling rates through weathering and degassing. This carbonate build-up is a missing factor in models of Earth's coupled climate, nutrient and oxygen evolution and is important for reconstructing Earth's history and potential exoplanet biogeochemistry.

Understanding Earth's gradual oxygenation tests the planetary boundary conditions that permit intelligent life. Earth's oxygenation included at least two broad steps: the Great Oxidation Event (GOE; 2.4–2.2 Ga (refs. 1,2)) and the Paleozoic Oxygenation Event (~450–400 Ma (refs. 3,4)) with mixed evidence for an intermediate step or period of instability during the Neoproterozoic Era (~800–540 Ma (refs. 5,6)). Studies have investigated the drivers of these events and to what degree they were driven by biological or geodynamic changes (for example, refs. 7,8).

The trajectory towards an oxygenated surface environment must have been driven by a rise in molecular oxygen (O_2) production or a decline in its consumption or a combination of both. Long-term photosynthetic oxygen production depends on the availability of the limiting nutrient phosphate[9], therefore increasing bioavailable phosphorus fluxes from the continents to the oceans are widely postulated to have driven oxygenation, for example, due to increasingly exposed continental landmass (for example, ref. 10) or enhanced weathering driven by the evolution of land plants (for example, ref. 11). A decline in reductant availability on Earth's surface is also a potential driver of oxygenation, either in discrete steps through volcanic regime changes[12] or changes in the oxidation state of volcanic and hydrothermal outputs[1].

[1]Yale Institute for Biospheric Studies, Yale University, New Haven, CT, USA. [2]Department of Earth and Planetary Sciences, Yale University, New Haven, CT, USA. [3]Ecohydrology Research Group, Water Institute and Department of Earth and Environmental Sciences, University of Waterloo, Waterloo, Ontario, Canada. [4]Institute of Astronomy, University of Cambridge, Cambridge, UK. [5]Department of Earth Sciences, Institute fur Geochemie und Petrologie, ETH Zurich, NW D 81.2, 5 Clausiusstrasse 25, Zurich, Switzerland. [6]Trinity College, University of Cambridge, Cambridge, UK. [7]Department of Earth Sciences, University of Cambridge, Cambridge, UK. [8]School of Earth and Environment, University of Leeds, Leeds, UK. [9]Present address: Now at School of Earth Sciences, University of Bristol, Bristol, UK. ✉e-mail: lewis.alcott@bristol.ac.uk
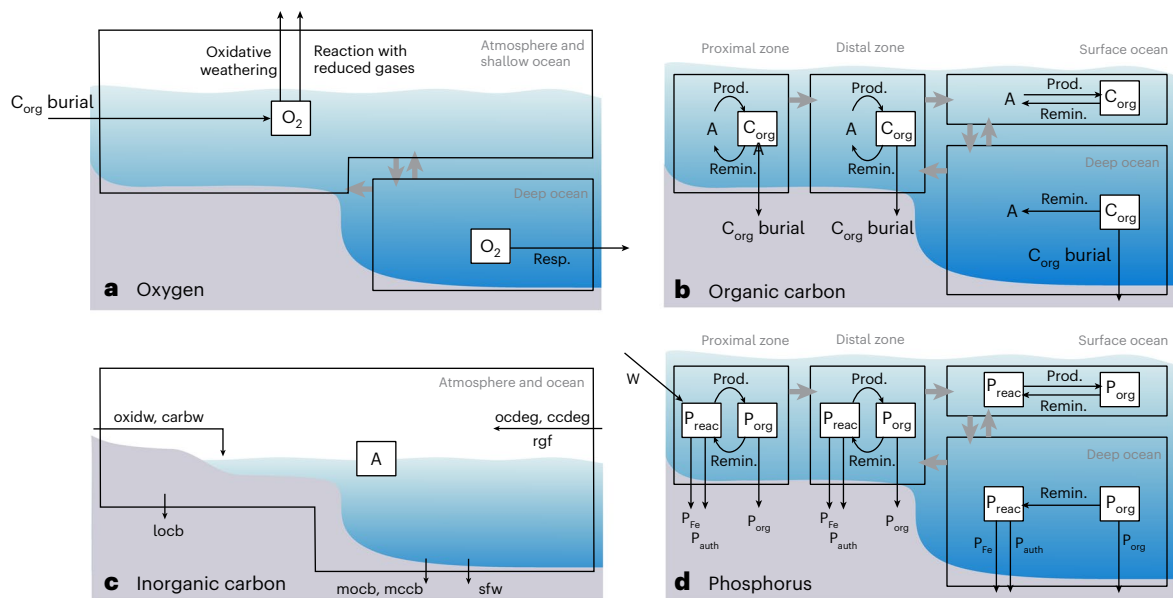
Fig. 1 | Model structure. a, Oxygen cycle, where the two boxes separate the deep ocean (bottom) from the well-mixed upper surface ocean and atmosphere (top). Resp., respiration. **b**, Organic carbon (C_{org}) cycle. Prod., primary productivity; Remin., remineralization. Fluxes to A denote exchange to the inorganic carbon reservoir, where A is the inorganic carbon reservoir. The primary production of organic carbon is taken from a singular reservoir of inorganic carbon. **c**, Inorganic carbon cycle, defined by a single box containing the atmosphere and oceans. Oxidw, oxidative weathering; carbw, carbonate weathering; locb, land organic

carbon burial; mocb, marine organic carbon burial; mccb, marine carbonate carbon burial; sfw, seafloor weathering; ocdeg, organic carbon degassing; ccdeg, carbonate carbon degassing; rgf, reduced gas flux. **d**, Phosphorus cycle, where P exists as soluble reactive phosphorus (P_{reac}) and organic bound phosphorus (P_{org}). Burial sinks of reactive phosphorus include iron bound P (P_{Fe}) and authigenic P phases (P_{auth}). The boxes with background blue background show hydrospheric reservoirs. The grey arrows denote mixing between them, and the black arrows denote biogeochemical fluxes.

The above source and sink arguments are reasonable and self-consistent, but the roles they play relative to each other in the combined carbon, oxygen and phosphorus cycles has not been established. Recent modelling shows that the broad oxygenation history of Earth can be suitably reproduced by either increasing the oxygen source or decreasing oxygen sinks over Earth's history[7].

Developing a theoretical understanding of the combined atmospheric and oceanic oxygen sources and sinks over Earth's history is challenging. One challenge is the regulation of surface temperature and CO_2 by temperature-dependent silicate weathering[13]. Here the global weathering rate adjusts to match the rate of CO_2 degassing, but this potentially results in extreme silicate weathering rates on the early Earth (if degassing rates were high) and a high rate of phosphate delivery and O_2 production.

A further complication is the carbonate $\delta^{13}C$ isotope record. This isotopic ratio is a product of changing carbon inputs and burial rates of inorganic and organic carbon. The record shows relative stability through all of Earth's history, with no large secular trends, invoking relatively invariable organic carbon burial and oxygen production[1,14], potentially requiring a decline in O_2 sink fluxes to explain oxygenation[12,15]. However, recent work determines that input of the lighter isotope would have been curtailed through restricted organic matter weathering on the anoxic ancient Earth; thus, the static $\delta^{13}C$ record may be reconciled with rising primary productivity over Earth's history[16-18].

Given recent advances, a consistent quantitative model for the evolution of Earth's carbon, oxygen and phosphorus cycles seems possible. In this Article, we develop a version of this (Fig. 1). The structure of this model is based on the five-box ocean and atmosphere model of Alcott et al.[7], with additions of an inorganic carbon cycle and simple climate based on the carbon, oxygen, phosphorus, sulfur and evolution (COPSE) model[19,20], allowing the model to dynamically calculate surface temperature, continental weathering rates and carbon isotope ratios. This new model does not permit fixing major components of the oxygen cycle, which are instead determined by the underlying

tectonics and model climate (see Supplementary Information for the model description).

Modelling the Earth system

Our model produces an emergent planetary state based on a small set of boundary conditions (Fig. 2). These initially include tectonic degassing of CO_2, exposure of the continents and possible biotic enhancement of weathering from the Paleozoic-present due to plant colonisation (Fig. 2a–c). Most studies propose a decline in degassing rates over Earth's history due to mantle cooling[21]. We use the estimate of Hayes and Waldbauer[22], with a 25–200% uncertainty window. Several different reconstructions are proposed for the exposure of subaerial landmass throughout Earth's history[23-25], so we adopt the Monte-Carlo parameter range used by Krissansen-Totten et al.[26] and add possible high-landmass options for the Archean. Increasing weathering efficiency due to the rise of land plants is also poorly constrained, and we also use the Monte-Carlo range of this parameter from Krissansen-Totten et al.[26], with the maximum change following the COPSE model[19] and the minimum assuming no enhancement.

We also vary the extent of phosphorus recycling in anoxic marine settings, testing C:P ratios of sedimentary organic matter overlain by anoxic water between 106 and 1,100, representing either no release or substantial preferential release[27] of phosphorus from these sediments and generally proposed to be associated with ferruginous or euxinic settings, respectively. Higher biomass C:P ratios (up to 300 (ref. 28)) may potentially occur under P-limited conditions during the Proterozoic, but we do not consider this independently. The model is run 1,000 times, subject to a random distribution of these parameter choices and initially using only forcings from Fig. 2a–c, with results shown in Fig. 3. Despite some encouraging results, such as the stability of carbonate $\delta^{13}C$, several major issues arise where the model cannot fit the long-term geological record.

These effects are generally caused by elevated carbon outgassing[22] and rapid weathering of fossil organic carbon (due to high O_2
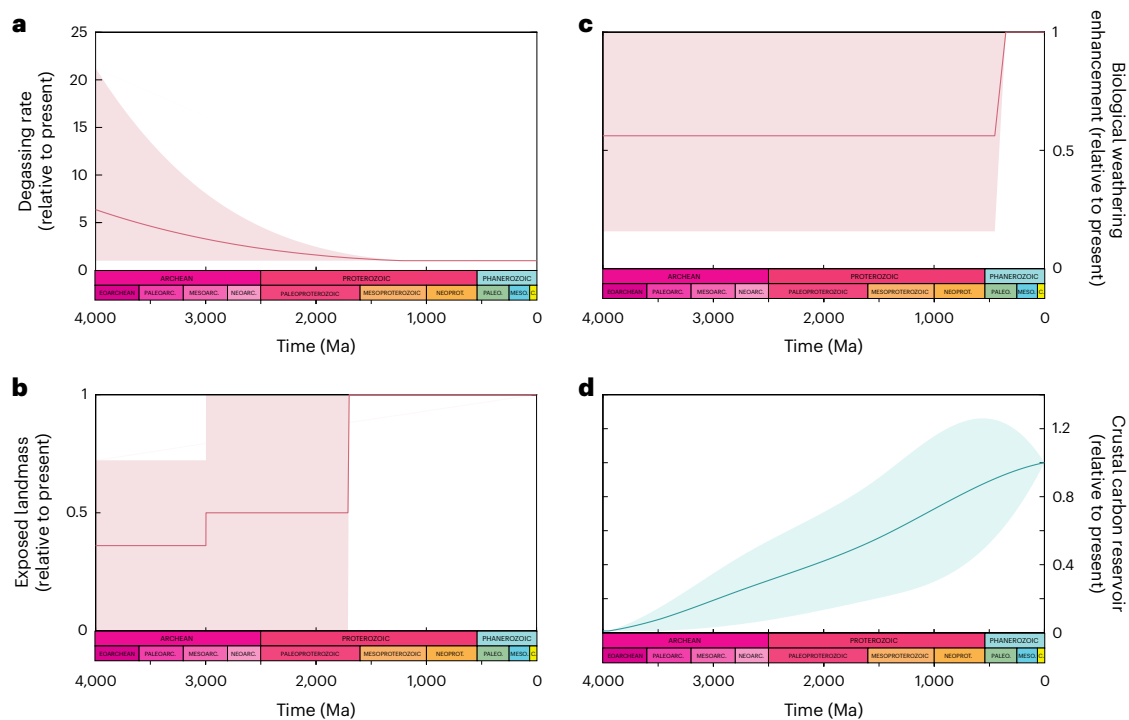
Fig. 2 | Model input parameters. a, The degassing rate[22]. **b**, Exposed landmass, relative to present[26]. **c**, Biological weathering enhancement[52]. **d**, Crustal carbon reservoir, relative to present[38,39]. The red and blue colours are used to highlight the difference between previously studied and newly studied parameters,

respectively. The darker lines show the mean values, and the shaded areas show assumed ranges. Paleoarc., Paleoarchean; Mesoarc., Mesoarchean; Neoarc., Neoarchean; Neoprot., Neoproterozoic; Paleo., Paleozoic; Meso., Mesozoic; C., Cenozoic.

and organic C burial), which together lead to higher CO_2 and surface temperature than the proxies suggest[26,29]. The uncertainty window does allow for static degassing rates over time[30], which is still insufficient to bring the model in line with the geological record. While such high temperatures are incompatible with the evidence for glaciation in the Archean and Paleoproterozoic, they are potentially supported by evidence for low-viscosity Archean oceans[31] and silicon isotopes[32], so they are not sufficient alone to falsify the model over long timescales. Our model uses a simple dimensionless climate approximation, but the CO_2–temperature relationships are broadly similar to climate models for the Archean[33], which were tested up to 0.2 bar CO_2. For CO_2 levels above this, our estimates become less accurate, and falsifying the results becomes more difficult.

A clearer mismatch between the model and data is atmospheric oxygen. There is strong evidence for less than 1 ppm atmospheric O_2 during the Archean[34], which is sufficient to falsify this version of the model. While a more accurate approximation of temperature may act to change the model oxygen level in the Archean, we can see that even when considering the lower end of the uncertainty range (which is supported by the GCM simulations), there are no low-oxygen solutions. A very high Archean reductant flux could potentially make this model consistent with the oxygenation record[7], but such high fluxes are contentious[29].

Introducing a crustal carbonate reservoir

We now explore an important mechanism that has not been included in coupled climate–oxygen–nutrient models for Earth's history. The primordial Earth had a silicate crust, but continual degassing of CO_2 and reactions with these silicate minerals has caused build-up of crustal carbonates over time, and they are now the largest store of crustal carbon[23,35]. An important consequence of this carbonate build-up is that continental rifts and arcs mobilize more carbon through metamorphism (hence why their activity has been linked to

greenhouse–icehouse climate cycles during the Phanerozoic[36]). Thus, an increasing crustal carbonate reservoir could imply a rising rate of CO_2 degassing, even if the mantle heat flow were to decrease substantially, or stay static, over time. This mechanism has been hypothesized to promote oxygenation[22,37], and previous modelling implied a trend towards oxygenation before the model breaks down[8], but it has not been included in a coupled model including carbon, nutrients and climate or been tested against combined geological data.

We parameterize carbonate build-up in our model using reconstructions of crustal sedimentary rocks[38,39]. The overall trends in crustal rock area, volume and lithological proportions with age in the reconstruction by Ronov[38] compare remarkably well with recent North American and global estimates from the Macrostrat geospatial database[40,41]. However, these databases do not track diffuse carbonate in siliciclastic sediments, which was probably more important in the past[42]. We also do not include carbonization of the seafloor[43,44] in our carbonate reservoir.

The model results with an accumulating crustal carbonate reservoir, in combination with the previously described input parameters, are shown in Fig. 4. This addition makes a critical difference to all model processes by gradually increasing the rate of carbon cycling through the ocean–atmosphere–crust system over geological time, thus reducing the carbon fluxes on the early Earth when compared with our previous model in Fig. 3. Here lower CO_2 degassing rates on the early Earth result in lower atmospheric CO_2 and temperature and reduced silicate weathering rates and nutrient delivery. This leads to lower rates of organic carbon burial and lower atmospheric O_2. Over long timescales, this also leads to less weathering of fossil organic carbon, further lowering CO_2 and maintaining carbonate $\delta^{13}C$ values close to zero.

We compare the model to the geological record to assess the reproduction of billion-year trends in multiple data sets—atmospheric and marine oxygen, atmospheric CO_2, average surface temperature,
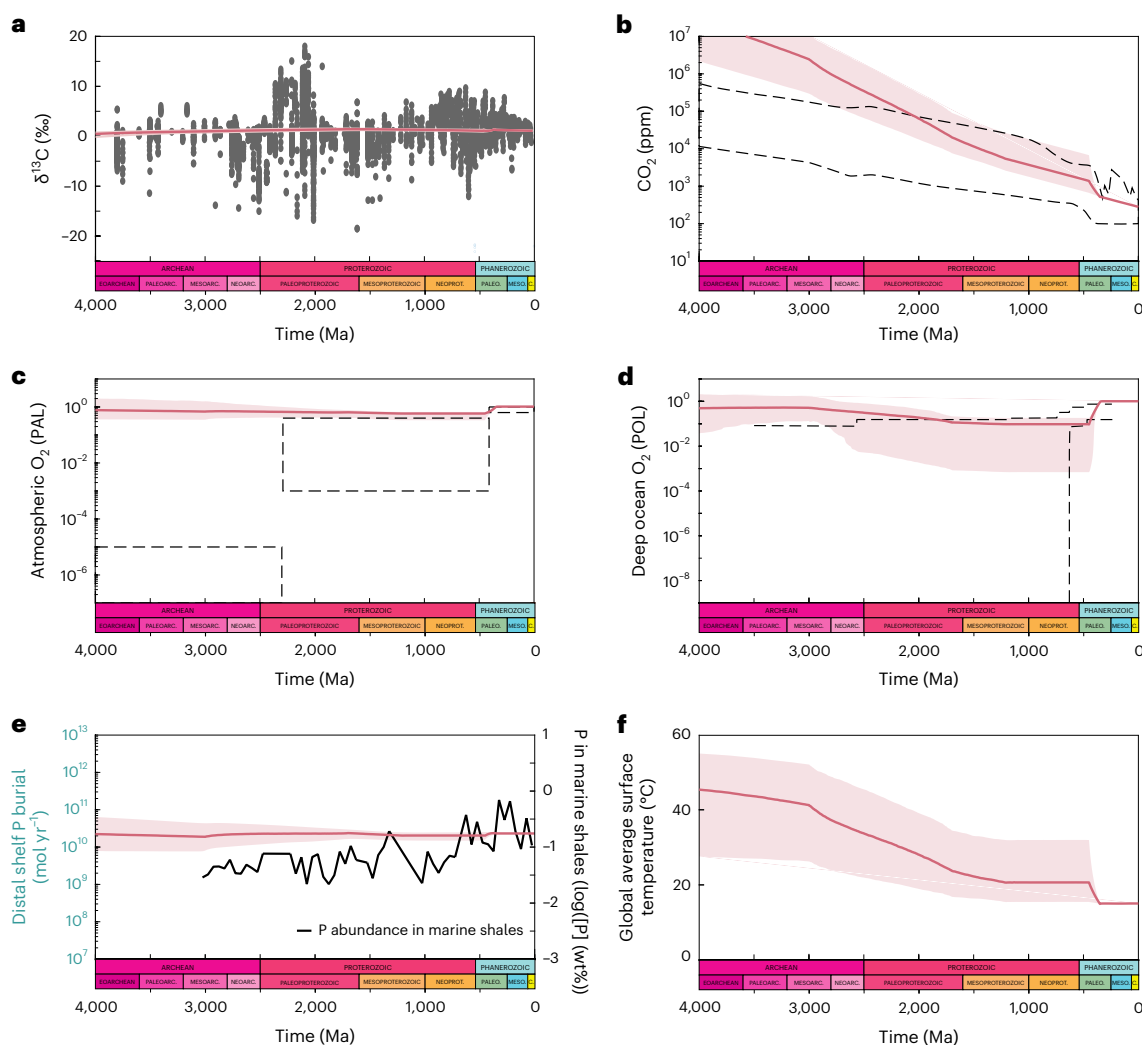
Fig. 3 | Model output with a fixed carbonate carbon reservoir. a, $\delta^{13}C$ of the atmosphere–ocean system plotted alongside carbonate isotope compilation from both Havig et al.[53] and Saltzman and Thomas[54]. **b**, CO_2 (ppm), with the dashed lines denoting the 95% confidence interval from a carbonate–silicate cycle model[29]. **c**, Atmospheric oxygen concentrations, with the dashed lines showing the oxygen concentrations from geochemical proxies[55,56]. **d**, Deep ocean oxygen content relative to present, with the dashed lines showing the oxygen

concentrations constrained by ophiolites[57]. POL, present ocean level. **e**, Total modelled phosphorus burial on the distal shelf. The black line shows the 50 Myr binned total phosphorus concentrations of shelf sediments[28]. **f**, Global average surface temperature in °C. The 95% confidence intervals are shown as a shaded area with the median value plotted. Paleoarc., Paleoarchean; Mesoarc., Mesoarchean; Neoarc., Neoarchean; Neoprot., Neoproterozoic; Paleo., Paleozoic; Meso., Mesozoic; C., Cenozoic.

carbon isotopes and sedimentary phosphorus abundance. The long timeframes result in greater data-model mismatch than is typical in studies of shorter timescales, however this multiproxy comparison remains a substantial challenge that has not previously been met. The billion-year $\delta^{13}C$ trend is famously invariant[45], and we consider our model output to be a good representation of this record, despite not producing large shorter-term excursions in the Paleoproterozoic and Phanerozoic, which are probably driven by mechanisms on shorter timescales than we consider. Similarly, the billion-year trend of the geological record of P in shales towards higher values[28] is now broadly captured.

A 'GOE' occurs in the model between ~3.5 and 2 Ga when reduced gas input is overwhelmed by oxygen production, and the primary regulation of oxygen switches to oxidative weathering[7,16]. This is a wide timeframe but covers the GOE interval at ~2.4 to 2.2 Ga (ref. 2), which is consistent with the billion-year evolution of the Earth. Subsequently, atmospheric oxygen concentrations in the Proterozoic and early Phanerozoic are between ~0.1% PAL (present atmospheric level) and ~75% PAL, before the advent of land plants. With the rise of land

plants O_2 is regulated close to present day levels[3,4]. Oceanic oxygen rises follow those of the atmosphere with an anoxic ($[O_2] < 1\ \mu mol\ l^{-1}$ in our model) deep ocean possible until the early Phanerozoic land plant colonization[5].

The modelled anoxic fraction of shelf seafloor has values of 20–90% for the Proterozoic and early Phanerozoic, with 30–80% anoxic for the Archean (Supplementary Fig. 1). Independent modelling suggests that ~15–50% of the surface ocean demonstrated quantifiable oxygen concentrations during the Archean[46], but these O_2 levels were low, and the simple Phanerozoic-based approximation we use for calculating anoxia probably underestimates the degree of anoxia for the Archean. We run a separate model where the anoxic fraction is fixed (Supplementary Fig. 2) to ensure this does not bias other model results. We do not simulate a 'Neoproterozoic Oxygenation Event' in either the atmosphere or ocean, but it is possible to have a stepwise shift in surface O_2 levels or a series of oxygen pulses within our model uncertainty range. The range permits an approximate fivefold increase in atmospheric O_2 during the Neoproterozoic and at least an order of magnitude increase in ocean oxygen content. However, much recent
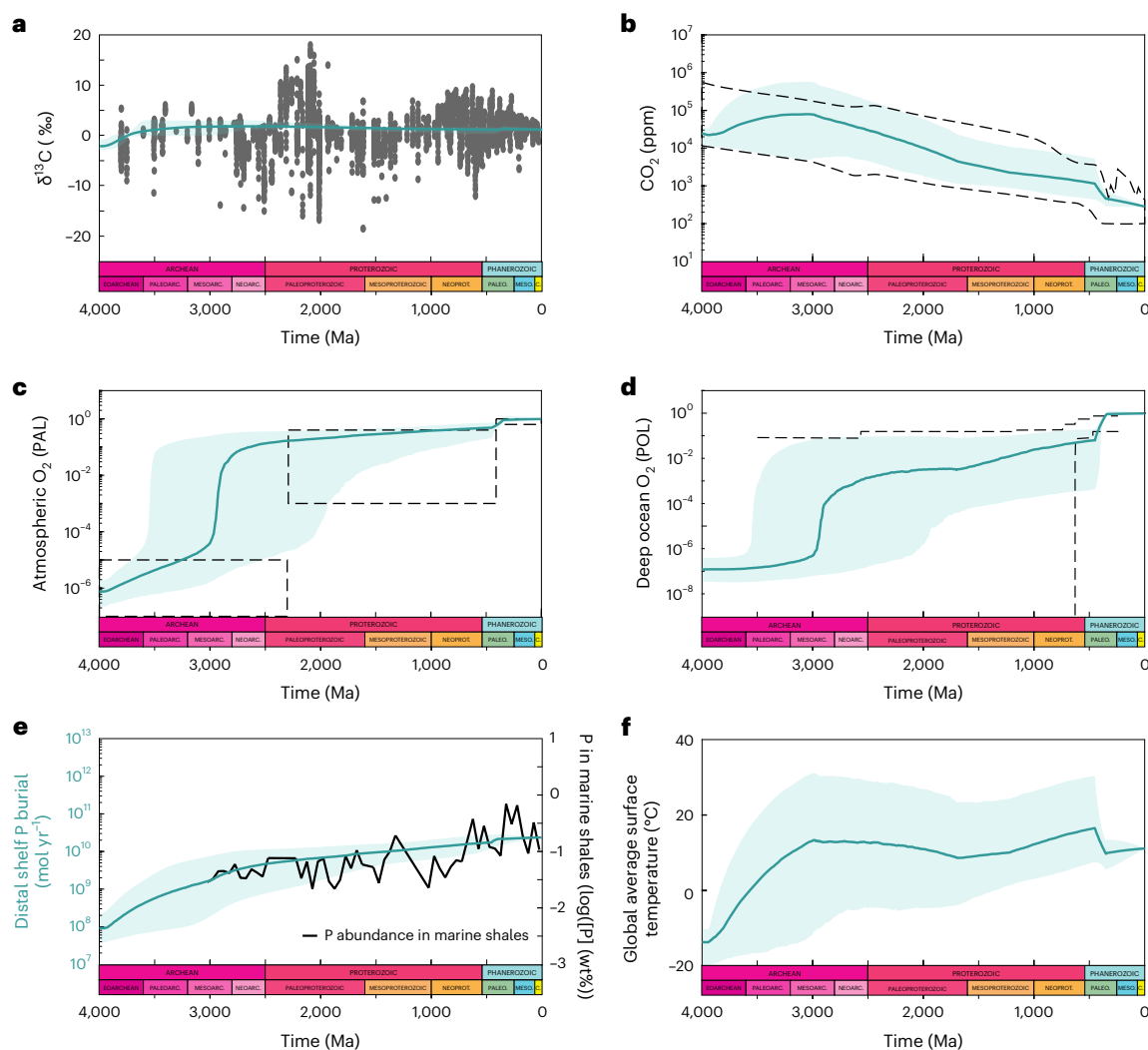
Fig. 4 | Standard run. a, $\delta^{13}C$ of atmosphere–ocean system plotted alongside carbonate isotope compilation from both Havig et al.[53] and Saltzman and Thomas[54]. **b**, CO_2 (ppm), with the dashed lines denoting the 95% confidence interval from a carbonate–silicate cycle model[29]. **c**, Atmospheric oxygen concentrations, with the dashed lines showing the oxygen concentrations from geochemical proxies[55,56]. **d**, Deep ocean oxygen content relative to present, with the dashed lines showing the oxygen concentrations constrained by ophiolites[57].

POL, present ocean level. **e**, Total modelled phosphorus burial on the distal shelf. The black line shows the 50 Myr binned total phosphorus concentrations of shelf sediments[28]. **f**, Global average surface temperature in °C. The 95% confidence intervals are shown as a shaded area with the median value plotted. Paleoarc., Paleoarchean; Mesoarc., Mesoarchean; Neoarc., Neoarchean; Neoprot., Neoproterozoic; Paleo., Paleozoic; Meso., Mesozoic; C., Cenozoic.

work is moving away from the idea of a stepwise change in Neoproterozoic oxygen levels[5,20,47].

Modelled CO_2 concentration falls within previously derived bounds[29] and global average surface temperature is between ~0 °C and ~30 °C over most of Earth's history. We produce very low surface temperatures in the Eoarchean due to crustal carbonate degassing tending to zero at this time. This is an interesting problem in itself and may simply be solved by the inclusion of other greenhouses gases, such as CH_4 (ref. 33), but the Eoarchean in general is outside the scope of the analysis in this paper, given the uncertainty about early tectonics and metabolisms.

In Supplementary Information we explore the model 'burial efficiency' of organic carbon (Supplementary Fig. 4), denoted here as the fraction of export production that is ultimately buried. We generally predicted this to be higher than present during the Precambrian due to lower O_2 levels and restricted respiration (Supplementary Fig. 4). Altering the model respiration rates allows us to explore changes in the burial efficiency. We find that a large range of marine oxygen levels is possible in this way (following Zhao et al.[48]), but the atmospheric

oxygen levels are much less affected because high burial efficiencies remove more phosphorus and, therefore, act to lower export production, buffering against the increased carbon burial (Supplementary Fig. 5). We do not impose an accumulation of organic carbon in the crust or track the size of the buried organic carbon reservoir. In Supplementary Figs. 6 and 7, we plot organic carbon burial and weathering fluxes and show that our model suggests a rise in crustal organic carbon over time. Recycling of organic carbon to the surface consumes O_2, so the build-up of organic carbon slightly counteracts the build-up of carbonates in this way. We also consider what happens in the model if we prescribe an an empty crustal carbonate reservoir that does not accumulate over time (Supplementary Fig. 9). In line with the results shown in Figs. 3 and 4, the model with no carbonate accumulation maintains low degassing rates, low surface temperature and very low oxygen levels, which is a poor match to the geological record.

We have chosen to neglect other previously discussed mechanisms in our modelling, and we defend those assumptions here. First, the process of hydrogen escape may have been vital in driving the GOE by changing the redox balance of Earth's surface[15]. However, after the

GOE, the ozone layer would have greatly inhibited this process, so it should make little difference during most of the Proterozoic and the Phanerozoic and cannot drive progressive oxygenation in the way carbonate build-up can. Nevertheless, including this within the model may change the dynamics of the GOE. Second, input of phosphorus from seafloor weathering is not considered in the model runs shown here. While P is released from basalt during submarine weathering in both oxic and anoxic environments[48], modern day oxic hydrothermal systems constitute an overall sink for P due to combination with iron or carbonate minerals[28]. It is unclear if anoxic hydrothermal systems are net producers or removers of P, especially as P drawdown has been widely documented in combination with iron minerals in anoxic settings[49]. Given this uncertainty, we model seafloor weathering as neither a source or sink of P in the manuscript, and we experiment instead with adding a maximum P flux from seafloor weathering in Supplementary Information (Supplementary Fig. 8), showing that this addition does not invalidate our conclusions. Finally, at the present day, anoxygenic photosynthesis contributes approximately 0.17% towards total productivity, but this may have been more important in the deep past[50]. We do not include the process here as it is generally believed that oxygenic photosynthesis had evolved before the GOE[34], but future work might uncover interesting dynamics associated with anoxygenic photosynthesis[51]. Finally, aside from the evolution of plants, we do not consider potential evolutionary mechanisms that may have altered the relationship between atmospheric CO_2, nutrient inputs and carbon burial. We assume a phosphate-limited photosynthetic biosphere throughout the entire model run. This is in line with most global biogeochemical models for these timeframes[7,9,16,49], but we hope that this work can contribute to subsequent investigation of alternative ideas. Clearly, without oxygenic photosynthesis, atmospheric O_2 would have remained low in the Hadean even under high nutrient inputs.

Implications for Earth's history

To summarize, we have constructed a self-consistent long-term model of the evolution of Earth's carbon, oxygen and phosphorus cycles, which is capable of reproducing the broad observed changes in atmosphere and ocean O_2 levels, atmospheric CO_2, carbonate carbon isotopes, global average surface temperature and phosphorus burial rates over Earth's history. This has not been done before, and by conducting this analysis, we have discovered that a critical missing component in models of the long-term Earth system is the build-up of carbonate minerals in Earth's crust, which results in increasing rates of carbon recycling over billion-year timescales. An increasing rate of carbon recycling resolves a problematic issue with quantitative reconstruction of Earth's key biogeochemical cycles over deep time, and it allows for constantly increasing rates of nutrient delivery from weathering, as well as a broadly static input rate of CO_2 into the surface system, despite a cooling mantle.

According to our numerical work, complete oxygenation of the Earth's surface was inevitable as soon as recycling of carbon was established, and oxygenic photosynthesis evolved. Continual degassing of the mantle CO_2 and deposition of carbonates has resulted in ever-increasing rates of carbon and nutrient cycling between the hydrosphere and crust[22], gradually increasing O_2 levels in the atmosphere and oceans. The observed step-change at the GOE is not clearly constrained in time by our work but must occur once the O_2 sources overwhelm sinks. We do not predict a distinct Neoproterozoic oxygenation, but the sporadic oxygenation observed in the geochemical record[20] and in independent modelling studies[6] is clearly possible within this framework, and even a relatively large step-change is possible within our model uncertainty envelope. The evolution of land plants acts to increase O_2 levels in our model. However, it appears that the continual burial and recycling of carbonates may have eventually led to a high-oxygen world without them.

This work has both positive and negative implications for the likelihood of aerobic, complex life existing on other worlds. On one side, we can create an oxygenated world in our model without needing a succession of specific tectonic or biological events to do so, meaning that one might expect more photosynthetic Earth-like planets, with an atmosphere, ocean and active crustal recycling, to be oxygen-rich. However, the long timeframe of carbonate build-up on Earth implies that an oxygen-dependent biosphere could have been stymied on a similar sized rocky planet until billions of years after planetary formation, thus it may be more probable that intelligence is restricted to older worlds or those with styles of crustal recycling permissive to more rapid build-up of crustal carbon inventories.

Online content

Any methods, additional references, Nature Portfolio reporting summaries, source data, extended data, supplementary information, acknowledgements, peer review information; details of author contributions and competing interests; and statements of data and code availability are available at https://doi.org/10.1038/s41561-024-01417-1.

References

1. Holland, H. D. Volcanic gases, black smokers, and the great oxidation event. *Geochim. Cosmochim. Acta* **66**, 3811–3826 (2002).
2. Poulton, S. W. et al. A 200-million-year delay in permanent atmospheric oxygenation. *Nature* **592**, 232–236 (2021).
3. Dahl, T. W. et al. Devonian rise in atmospheric oxygen correlated to the radiations of terrestrial plants and large predatory fish. *Proc. Natl Acad. Sci. USA* **107**, 17911–17915 (2010).
4. Krause, A. J. et al. Stepwise oxygenation of the Paleozoic atmosphere. *Nat. Commun.* **9**, 4081 (2018).
5. Sperling, E. A. et al. Statistical analysis of iron geochemical data suggests limited late Proterozoic oxygenation. *Nature* **523**, 451–454 (2015).
6. Krause, A. J., Mills, B. J. W., Merdith, A. S., Lenton, T. M. & Poulton, S. W. Extreme variability in atmospheric oxygen levels in the late Precambrian. *Sci. Adv.* **8**, eabm8191 (2022).
7. Alcott, L. J., Mills, B. J. W. & Poulton, S. W. Stepwise Earth oxygenation is an inherent property of global biogeochemical cycling. *Science* **366**, 1333–1337 (2019).
8. Lee, C. A. et al. Two-step rise of atmospheric oxygen linked to the growth of continents. *Nat. Geosci.* https://doi.org/10.1038/ngeo2707 (2016).
9. Tyrrell, T. The relative influences of nitrogen and phosphorus on oceanic primary production. *Nature* **400**, 525–531 (1999).
10. Campbell, I. H. & Allen, C. M. Formation of supercontinents linked to increases in atmospheric oxygen. *Nat. Geosci.* https://doi.org/10.1038/ngeo259 (2008).
11. Lenton, T. M. et al. Earliest land plants created modern levels of atmospheric oxygen. *Proc. Natl Acad. Sci. USA* **113**, 9704–9709 (2016).
12. Kump, L. R. & Barley, M. E. Increased subaerial volcanism and the rise of atmospheric oxygen 2.5 billion years ago. *Nature* **448**, 1033–1036 (2007).
13. Walker, J. C. G., Hays, P. B. & Kasting, J. F. A negative feedback mechanism for the long-term stabilization of Earth's surface temperature. *J. Geophys. Res.* https://doi.org/10.1029/JC086iC10p09776 (1981).
14. Rothman, D. H. Earth's carbon cycle: a mathematical perspective. *Bull. Am. Math. Soc.* **52**, 47–64 (2015).
15. Catling, D. C., Zahnle, K. J. & McKay, C. Biogenic methane, hydrogen escape, and the irreversible oxidation of early Earth. *Science* **293**, 839–843 (2001).
16. Daines, S. J., Mills, B. J. W. & Lenton, T. M. Atmospheric oxygen regulation at low Proterozoic levels by incomplete oxidative weathering of sedimentary organic carbon. *Nat. Commun.* **8**, 14379 (2017).

17. Krissansen-Totton, J., Kipp, M. & Catling, D. C. Inverse modeling of carbon isotope record suggests changes in organic burial could explain Great Oxidation Event. *Geobiology* https://doi.org/10.1111/gbi.12440 (2021).

18. Planavsky, N. J. et al. On carbon burial and net primary production through Earth's history. *Am. J. Sci.* **322**, 413–460 (2022).

19. Lenton, T. M., Daines, S. J. & Mills, B. J. W. COPSE reloaded: an improved model of biogeochemical cycling over Phanerozoic time. *Earth Sci. Rev.* **178**, 1–28 (2018).

20. Tostevin, R. & Mills, B. J. W. Reconciling proxy records and models of Earth's oxygenation during the Neoproterozoic and Palaeozoic. *Interface Focus* **10**, 20190137 (2020).

21. Sleep, N. H. & Zahnle, K. J. Carbon dioxide cycling and implications for climate on ancient Earth. *J. Geophys. Res. Planets* https://doi.org/10.1029/2000JE001247 (2001).

22. Hayes, J. M. & Waldbauer, J. R. The carbon cycle and associated redox processes through time. *Philos. Trans. R. Soc. B* **361**, 931–950 (2006).

23. Armstrong, R. L. Radiogenic isotopes: the case for crustal recycling on a near-steady-state no continental-growth Earth. *Philos. Trans. R. Soc. Lond. A* **301**, 443–472 (1981).

24. Campbell, I. H. Constraints on continental growth models from Nb/U ratios in the 3.5 Ga Barberton and other Archaean basalt-komatiite suites. *Am. J. Sci.* **303**, 319–351 (2003).

25. Johnson, B. W. & Wing, B. A. Limited Archaean continental emergence reflected in an early Archaean 18O-enriched ocean. *Nat. Geosci.* **13**, 243–248 (2020).

26. Krissansen-Totton, J., Arney, G. N. & Catling, D. C. Constraining the climate and ocean pH of the early Earth with a geological carbon cycle model. *Proc. Natl Acad. Sci. USA* **115**, 4105–4110 (2018).

27. Slomp, C. P., Thomson, J. & de Lange, G. J. Controls on phosphorus regeneration and burial during formation of eastern Mediterranean sapropels. *Mar. Geol.* **203**, 141–159 (2004).

28. Reinhard, C. T. et al. Evolution of the global phosphorus cycle. *Nature* **541**, 386–389 (2017).

29. Catling, D. C. & Zahnle, K. J. The Archean atmosphere. *Sci. Adv.* **6**, eaax1420 (2020).

30. Korenaga, J. Plate tectonics, flood basalts and the evolution of Earth's oceans. *Terra Nova* **20**, 419–439 (2008).

31. Fralick, P. & Carter, J. E. Neoarchean deep marine paleotemperature: evidence from turbidite successions. *Precambrian Res.* **191**, 78–84 (2011).

32. Robert, F. & Chaussidon, M. A palaeotemperature curve for the Precambrian oceans based on silicon isotopes in cherts. *Nature* **443**, 969–972 (2006).

33. Wolf, E. T. & Toon, O. B. Hospitable Archean climates simulated by a general circulation model. *Astrobiology* **13**, 1–18 (2013).

34. Lyons, T. W., Reinhard, C. T. & Planavsky, N. J. The rise of oxygen in Earth's early ocean and atmosphere. *Nature* **506**, 307–315 (2014).

35. Duncan, M. S. & Dasgupta, R. Rise of Earth's atmospheric oxygen controlled by efficient subduction of organic carbon. *Nat. Geosci.* **10**, 387–392 (2017).

36. McKenzie, N. R. et al. Continental arc volcanism as the principal driver of icehouse-greenhouse variability. *Science* **352**, 444–447 (2016).

37. Holland, H. D. Why the atmosphere became oxygenated: a proposal. *Geochimica Cosmochimica Acta* **73**, 5241–5255 (2009).

38. Ronov, A. B. General trends in the composition of the crust, ocean, and atmosphere. *Geokhimya* **8**, 714–743 (1964).

39. Veizer, J. & MacKenzie, F. T. Evolution of sedimentary rocks. *Treatise Geochem.* **7**, 239–407 (2003).

40. Peters, S. E. & Husson, J. M. Sediment cycling on continental and oceanic crust. *Geology* **45**, 323–326 (2017).

41. Peters, S. E. et al. Igneous rock area and age in continental crust. *Geology* **49**, 1235–1239 (2021).

42. Wang, J., Tarhan, L. G., Jacobson, A. D., Oehlert, A. M. & Planavsky, N. J. The evolution of the marine carbonate factory. *Nature* **615**, 265–269 (2023).

43. Plank, T. & Manning, C. E. Subducting carbon. *Nature* **574**, 343–352 (2019).

44. Thomson, A. R., Walter, M. J., Kohn, S. C. & Brooker, R. A. Slab melting as a barrier to deep carbon subduction. *Nature* **529**, 76–79 (2016).

45. Schidlowski, M. A 3,800-million-year isotopic record of life from carbon in sedimentary rocks. *Nature* **333**, 313–318 (1988).

46. Olson, S. L., Kump, L. R. & Kasting, J. F. Quantifying the areal extent and dissolved oxygen concentrations of Archean oxygen oases. *Chem. Geol.* **362**, 35–43 (2013).

47. Luo, J. et al. Pulsed oxygenation events drove progressive oxygenation of the early Mesoproterozoic ocean. *Earth Planet. Sci. Lett.* **559**, 116754 (2021).

48. Syverson, D. D. et al. Nutrient supply to planetary biospheres from anoxic weathering of mafic oceanic crust. *Geophys. Res. Lett.* https://doi.org/10.1029/2021GL094442 (2021).

49. Alcott, L. J., Mills, B. J. W., Bekker, A. & Poulton, S. W. Earth's Great Oxidation Event facilitated by the rise of sedimentary phosphorus recycling. *Nat. Geosci.* **15**, 210–215 (2022).

50. Johnston, D. T., Wolfe-Simon, F., Pearson, A. & Knoll, A. H. Anoxygenic photosynthesis modulated Proterozoic oxygen and sustained Earth's middle age. *Proc. Natl Acad. Sci. USA* **106**, 16925–16929 (2009).

51. Jones, C., Nomosatryo, S., Crowe, S. A., Bjerrum, C. J. & Canfield, D. E. Iron oxides, divalent cations, silica, and the early earth phosphorus crisis. *Geology* **43**, 135–138 (2015).

52. Bergman, N. M., Lenton, T. M. & Watson, A. J. COPSE: a new model of biogeochemical cycling over Phanerozoic time. *Am. J. Sci.* **304**, 397–437 (2004).

53. Havig, J. R., Hamilton, T. L., Bachan, A. & Kump, L. R. Sulfur and carbon isotopic evidence for metabolic pathway evolution and a four-stepped Earth system progression across the Archean and Paleoproterozoic. *Earth Sci. Rev.* **174**, 1–21 (2017).

54. Saltzman, M. R. & Thomas, E. in *The Geological Time Scale*. Ch. 11 (eds Gradstein, F. M. et al.) 221–246 (Elsevier, 2012).

55. Kump, L. R. The rise of atmospheric oxygen. *Nature* **451**, 277–278 (2008).

56. Planavsky, N. J. et al. Low mid-Proterozoic atmospheric oxygen levels and the delayed rise of animals. *Science* **346**, 635–638 (2014).

57. Stolper, D. A. & Keller, C. B. A record of deep-ocean dissolved O_2 from the oxidation state of iron in submarine basalts. *Nature* **553**, 323–327 (2018).

Methods

The model developed here comprises the carbon, oxygen and phosphorus cycles across a five-box ocean and atmosphere system. The organic portion of this model is based on the model presented in Alcott et al.[7], while the inorganic carbon cycle is predominantly based on the COPSE family of models[19,20]. The framework of Alcott et al.[7] is retained with a four-box ocean and one-box atmosphere structure. The addition of the inorganic carbon cycle allows for simulation of atmospheric CO_2 concentrations, global average surface temperature and dynamic weathering fluxes for silicates, carbonates and phosphorus and fossil organic matter. This model is forced by a small set of key geological processes and tested by 1,000 Monte-Carlo simulations, with the maximum and minimum values defined by the geological record. The parameters varied include reduced gas flux[22], crustal carbonate carbon build-up[38,39], fraction of exposed landmass[26], anoxic sediment P recycling rate (denoted by C_{org}:P_{org} (ref. 27)) and land plant weathering enhancement[19] (Fig. 1). The full model description and equations can be found in Supplementary Information, and the code can be downloaded at ref. 58.

Data availability

Model data can be downloaded at GitHub (https://github.com/lalcott/d13Ctemp_2023) (ref. 58).

Code availability

Model code can be downloaded at GitHub (https://github.com/lalcott/d13Ctemp_2023) (ref. 58).

References

58.   *GitHub* (2024); https://github.com/lalcott/d13Ctemp_2023

Author contributions

L.J.A. and B.J.W.M. designed the research and conducted the modelling. All authors contributed to writing and reviewing the manuscript.

Competing interests

The authors declare no competing interests.

Additional information

Supplementary information The online version contains supplementary material available at https://doi.org/10.1038/s41561-024-01417-1.

Correspondence and requests for materials should be addressed to Lewis J. Alcott.

Peer review information *Nature Geoscience* thanks Eva Stüeken and the other, anonymous, reviewer(s) for their contribution to the peer review of this work. Primary Handling Editor: Alison Hunt, in collaboration with the *Nature Geoscience* team.

Reprints and permissions information is available at www.nature.com/reprints.